

Article

Electronic, Magnetic and Optical Properties of Double Perovskite Compounds: A First Principle Approach

Mehtab Ur Rehman , Qun Wang * and Yunfei Yu

Faculty of Materials and Manufacturing, Beijing University of Technology, No.100, Pingleyuan, Chaoyang District, Beijing 100000, China

* Correspondence: wangq@bjut.edu.cn

Abstract: Double perovskite compounds (DPCs) have gained much more attention due to their versatile character in the fields of electronics and spintronics. Using density functional theory (DFT) we investigated the electronic, magnetic and optical properties of DPC $A_2BB'O_6$ where $B = Cr, Sc$ and V and $B' = Co, Ni$. The electronic band gaps suggest these compounds are half-metallic (HF) semiconductors in the spin-up channel and metallic in the spin-down channel. Magnetic properties suggest these are ferromagnetic in nature, so all DPCs are half-metallic ferromagnetic (HM-FM). Furthermore, the compound La_2CrCoO_6 shows outstanding electronic and optical properties, so it can be used in optoelectronic/spintronic devices.

Keywords: DFT; double perovskite; electronic; magnetic; optical conductivity



Citation: Rehman, M.U.; Wang, Q.; Yu, Y. Electronic, Magnetic and Optical Properties of Double Perovskite Compounds: A First Principle Approach. *Crystals* **2022**, *12*, 1597. <https://doi.org/10.3390/cryst12111597>

Academic Editor: Wen-Ching Hsieh

Received: 17 September 2022

Accepted: 31 October 2022

Published: 10 November 2022

Publisher's Note: MDPI stays neutral with regard to jurisdictional claims in published maps and institutional affiliations.



Copyright: © 2022 by the authors. Licensee MDPI, Basel, Switzerland. This article is an open access article distributed under the terms and conditions of the Creative Commons Attribution (CC BY) license (<https://creativecommons.org/licenses/by/4.0/>).

1. Introduction

Recently, double perovskite compounds (DPCs) have attracted researchers due to their outstanding properties in many applications [1,2]. The crystal structure of double perovskite can be derived out of an ordinary perovskite structure ABO_3 which has a wide range of properties starting from insulators to superconductors [3–7]. The perovskite structure has structure and flexibility, so almost all elements in the periodic table can be used in the form of a perovskite crystal structure [8]. The double perovskite compounds are composed of two simple perovskite structures (SPS), ABO_3 and ABO_3 , so the general chemical formula for DPCs is $A_2BB'O_6$. DPCs are formed when the half of cations of the B site are swapped by another cation B' , achieving rock salt ordering between these cations [9]. Figure 1a shows the simple perovskite crystal structure ABO_3 and part (b) shows the double perovskite structure composed of two SPS, $A_2BB'O_6$. Usually, in the double perovskite compound $A_2BB'O_6$, the A site is occupied by the elements of alkaline earth metals (Ca, Sr, Ba, etc.) or lanthanides (La) and the B and B' position are filled by the transition metal elements (Mn, Sc, Co, Ni, etc.) [10].

The transition metal ions (TMI) at B and B' in the DPS show a wide range of magnetic and electronic properties. The TMI is responsible for chemical flexibility and complex character, which associate with the coordination of TMI with oxygen [11].

In 2001, Hua and Wu studied the electronic and magnetic properties of the DPCs A_2FeReO_6 ($A = Ca, Sr$ and Ba), Sr_2MMoO_6 and ($M = Co, Fe, Cr$ and Mn) using the local spin density approximation (LSDA) and (LSDA + U). They reported that the compounds $BaFeReO_6$ and $SrFeReO_6$ are half-metallic ferrimagnetic (HM-FiM) due to spin-orbital coupling between Fe^{3+} and Re^{5+} . The compound Sr_2MMoO_6 has strong p-d covalency effects which cause the same valence state combinations [12].

In 2020, Mehtab ur Rehman and coworkers investigated the optoelectronic properties of the organic-inorganic perovskite, methyl-ammonium lead halide (MLH) $CH_3NH_3PbX_3$, ($X = Cl, Br$ and I) using DFT simulation. They concluded that all the compounds are semiconductors with band gaps of 1.98 eV, 2.36 eV and 2.78 eV for $CH_3NH_3PbI_3$, $CH_3NH_3PbBr_3$

and $\text{CH}_3\text{NH}_3\text{PbCl}_3$, respectively. The compound $\text{CH}_3\text{NH}_3\text{PbI}_3$ has a narrow band gap and is assumed to be the best candidate for optoelectronic applications [13].

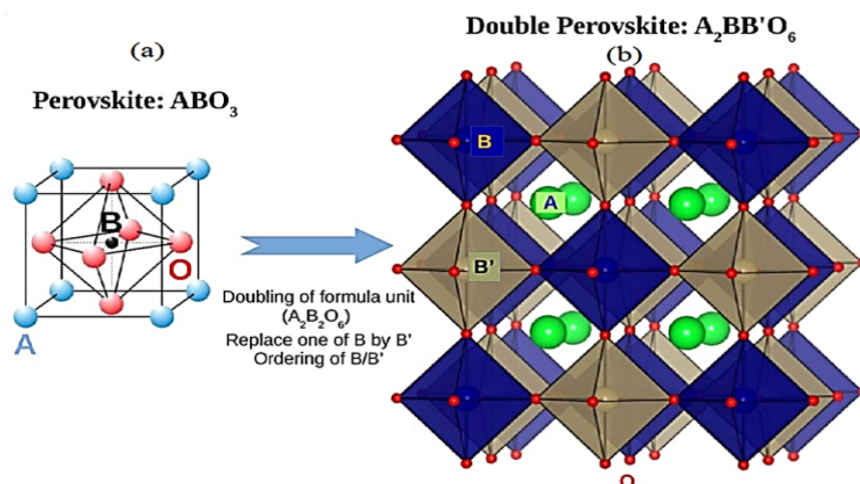


Figure 1. (a) Simple perovskite structure ABO_3 (b) double perovskite structure $\text{A}_2\text{BB}'\text{O}_6$.

Moreover, in 2021, Ghaithan Hamid M et al. investigated the optoelectronic properties of in-organic perovskite CsPbX_3 ($X = \text{I}, \text{Br}, \text{Cl}$) compounds using the DFT approach. They used inorganic structures because they have high thermal stability as compared to organic compounds. All of them are founded semiconductors with effective optical band gaps. Furthermore, their optical properties clarified that they are suitable for optoelectronic applications [14].

Additionally, in 2017, H. Kabbour et al. used a topochemical modification method and achieved an extreme reduction in the multiferroic material of the YMoO_3 perovskite structure. These are key materials for fabricating magnetic field sensors, actuators, switches and memory devices [15].

Later on, J. T. Homg and G. Y. Guo investigated the electronic and magnetic properties using LSDA and GGA methods of other DPC compounds Sr_2CrWO_6 , $\text{Sr}_2\text{FeReO}_6$ and $\text{Sr}_2\text{FeMoO}_6$. All compounds were found to be half-metallic ferromagnetic (HM-FM) in nature while the calculated total spin magnetic moment of Sr_2CrWO_6 , $\text{Sr}_2\text{FeReO}_6$ and $\text{Sr}_2\text{FeMoO}_6$ were $2 \mu\text{B}$, $3 \mu\text{B}$ and $4 \mu\text{B}$, respectively [16].

After that, K. L. Holman et al., in 2006, synthesized the Lanthanum-based DPCs La_2NiVO_6 , $\text{La}_2\text{CoTiO}_6$ and La_2CoVO_6 using the solid-state method. They reported that all of the La-based DPCs are semiconductors with band gaps of 0.41 eV, 0.45 eV and 1.02 eV of compounds La_2CoVO_6 , La_2NiVO_6 and $\text{La}_2\text{CoTiO}_6$, respectively [17].

Recently, the double perovskite compound $\text{Sr}_2\text{ZnTeO}_6$ was synthesized using the solid-state method and its optical and electronic properties were investigated. The crystal symmetry, phase formation, and purity were investigated with the help of X-ray diffraction (XRD) and the energy band gap of 4.11 eV was calculated using ultraviolet-visible light spectroscopy (UV-Vis). Therefore, there are a number of double perovskite compounds that have been synthesised and their properties were investigated using different techniques [18–20].

Likewise, recently, T. K. Bhowmik et al. synthesised the double perovskite compound $\text{La}_2\text{CrNiO}_6$ using the sol-gel method. They used many characterisation techniques to study the structural and electronic nature of the $\text{La}_2\text{CrNiO}_6$ compound. Structurally, the XRD data confirmed that $\text{La}_2\text{CrNiO}_6$ crystallises in the orthorhombic phase while electronically, the impedance spectroscopy in the temperature range between 30°C and 560°C with the frequency of 42 Hz–4.8 MHz justified that the compound is metallic in nature due to a decrease in conductivity with frequency in the experimental temperature range [21].

In this research, we calculated the electronic, magnetic and optical properties of the DPC $\text{La}_2\text{BB}'\text{O}_6$ where $B = \text{Cr}, \text{Sc}$ and V and $B' = \text{Co}, \text{Ni}$ using a first principle approach. The band structures, density of states, spin magnetic moments and optical parameters are

analysed. The optical properties are very important for these compounds because optically, the DPC structure is much less explored.

2. Methodology

In the present calculations, we used Wien2k software based on density functional theory (DFT). The structure optimisation and many physical properties of the DPC $\text{La}_2\text{BB}'\text{O}_6$ were carried out using generalised gradient approximation (GGA) and GGA+U scheme [22–25]. The GG+U (Hybrid term) is a famous approach to calculate electronic, magnetic and optical properties of transition metal oxides (strong metal system) [6,26]. In our calculations, we used both GGA and GGA+U approaches. Furthermore, the calculations were carried out with the ‘Full potential linearised augmented plane wave (FP-LAPW)’ approach implemented in Wien2k code. The radii of the muffin-tin sphere for the DPC $\text{La}_2\text{BB}'\text{O}_6$ are taken as $3.5 a_0$ for La, $2.0 a_0$ for transition metals Cr, Sc, Co, Ni and $1.5 a_0$ for O. The self-consistent field cycle (SCF) calculations convergence is attained at 0.7 mR_y as well as the convergence of charge $0.0001e$. All of the compounds are in a cubic structure, making a super cell ($2 \times 2 \times 1$) structure and relaxed atomic position till force convergence becomes $5 \times 10^{-3} \text{ eV/\AA}$ and energy approaches 10^{-4} eV . In the present calculations for better convergence of charge in the DMS, the wave cut-off value $R_{\text{mt}}K_{\text{max}} = 6$ in the interstitial region, 4000 k-points and $G_{\text{max}} = 24$ is taken.

3. Results and Discussions

The DPCs $\text{La}_2\text{CrCoO}_6$, $\text{La}_2\text{CrNiO}_6$, $\text{La}_2\text{ScNiO}_6$, La_2VNiO_6 and La_2VScO_6 electronic, magnetic and optical properties were analysed in a periodic manner and the figures were generated using XMGRACE software. The path of k-points in the band structure and density of states is taken as (Γ H N Γ P). All the compounds are semiconductors with spin-down channels and metallic for spin-up channels in GGA and GGA+U.

3.1. Band Structure Calculations

The band structures consist of the valence band (VB) and the conduction band (CB) and in between the energy gap E_g , the VB and CB are both crowded and overlapping in the spin-up channel, while there is a forbidden energy gap in the spin-down channel between them. All of the DPCs of $\text{La}_2\text{BB}'\text{O}_6$ are found to be direct band gap semiconductors because CB minima and VB maxima occur at the same point of symmetry in the Brillouin zone. Therefore, all DPCs of $\text{La}_2\text{BB}'\text{O}_6$ are metallic in the spin-up and semiconductors in the spin-down channel and are known as half-metallic double perovskite compounds (HM-DPC). The calculated band gaps in the spin-down channels using the GGA method are 0.94, 1.14, 1.63, 1.22 and 3.53 eV for $\text{La}_2\text{CrCoO}_6$, $\text{La}_2\text{CrNiO}_6$, $\text{La}_2\text{ScNiO}_6$, La_2VNiO_6 and La_2VScO_6 , respectively. The calculated band gaps in the spin-down channels using the GGA+U method are 1.66, 1.21, 3.85, 2.08 and 3.56 eV for $\text{La}_2\text{CrCoO}_6$, $\text{La}_2\text{CrNiO}_6$, $\text{La}_2\text{ScNiO}_6$, La_2VNiO_6 and La_2VScO_6 , respectively. All the calculated band gaps are in good agreement with previous theoretical findings, also discussed in Table 1 [6,27]. Figures 2 and 3 show all DPC band structures using GGA and GGA+U, respectively.

Table 1. Comparison of calculated electronic band gaps with previous electronic structure findings.

DPC	GGA (Current)		GGA+U (Current)		GGA (Other)		GGA+U (Other)	
	Spin-Up	Spin-Down	Spin-Up	Spin-Down	Spin-Up	Spin-Down	Spin-Up	Spin-Down
$\text{La}_2\text{CrCoO}_6$	Metallic	0.945 eV	Metallic	1.667 eV	Metallic	0.762 eV	Metallic	2.471 eV
$\text{La}_2\text{CrNiO}_6$	Metallic	1.149 eV	Metallic	1.211 eV	Metallic	1.007 eV	Metallic	3.293 eV
$\text{La}_2\text{ScNiO}_6$	Metallic	1.632 eV	Metallic	3.855 eV	Metallic	1.497 eV	Metallic	3.293 eV
La_2VNiO_6	Metallic	1.225 eV	Metallic	2.008 eV	Metallic	1.116 eV	Metallic	3.65 eV
La_2VScO_6	Metallic	3.537 eV	Metallic	3.566 eV	Metallic	3.238 eV	Metallic	3.238 eV

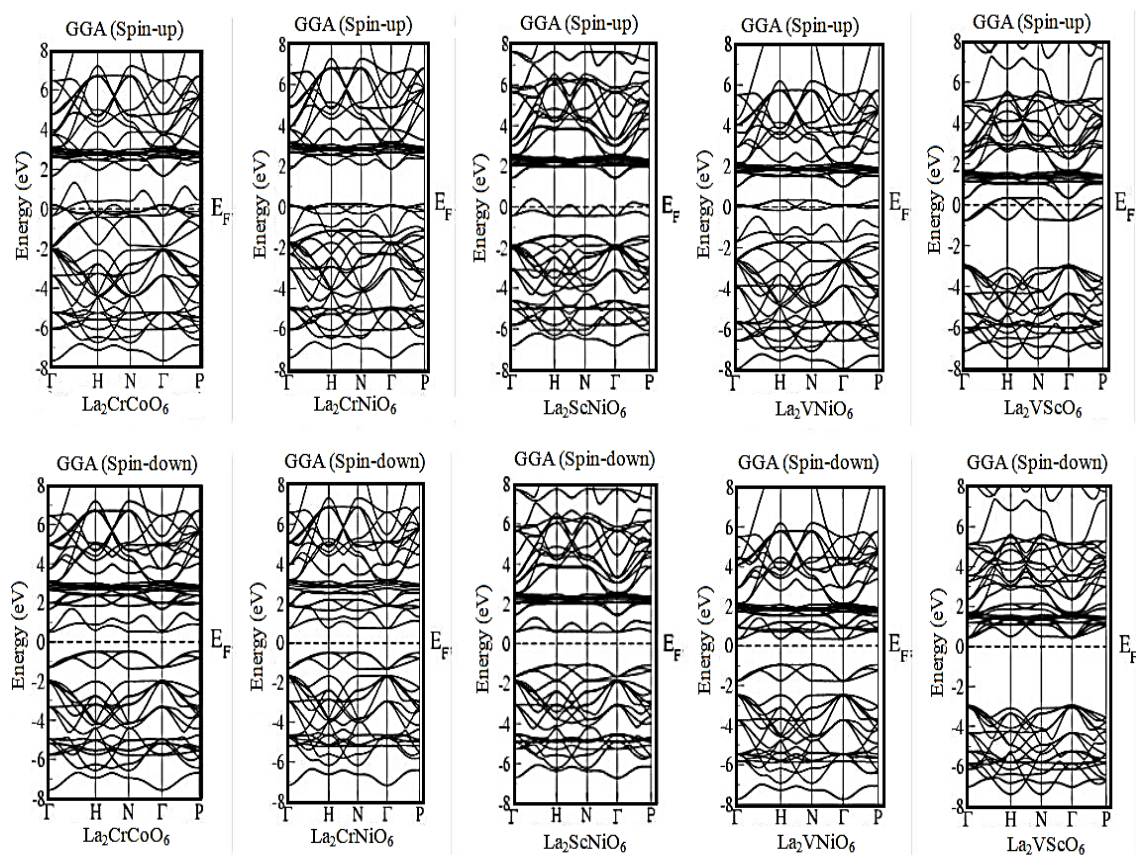


Figure 2. Band structures of DPC $\text{La}_2\text{BB}'\text{O}_6$ using GGA in both spin-up and spin-down channels.

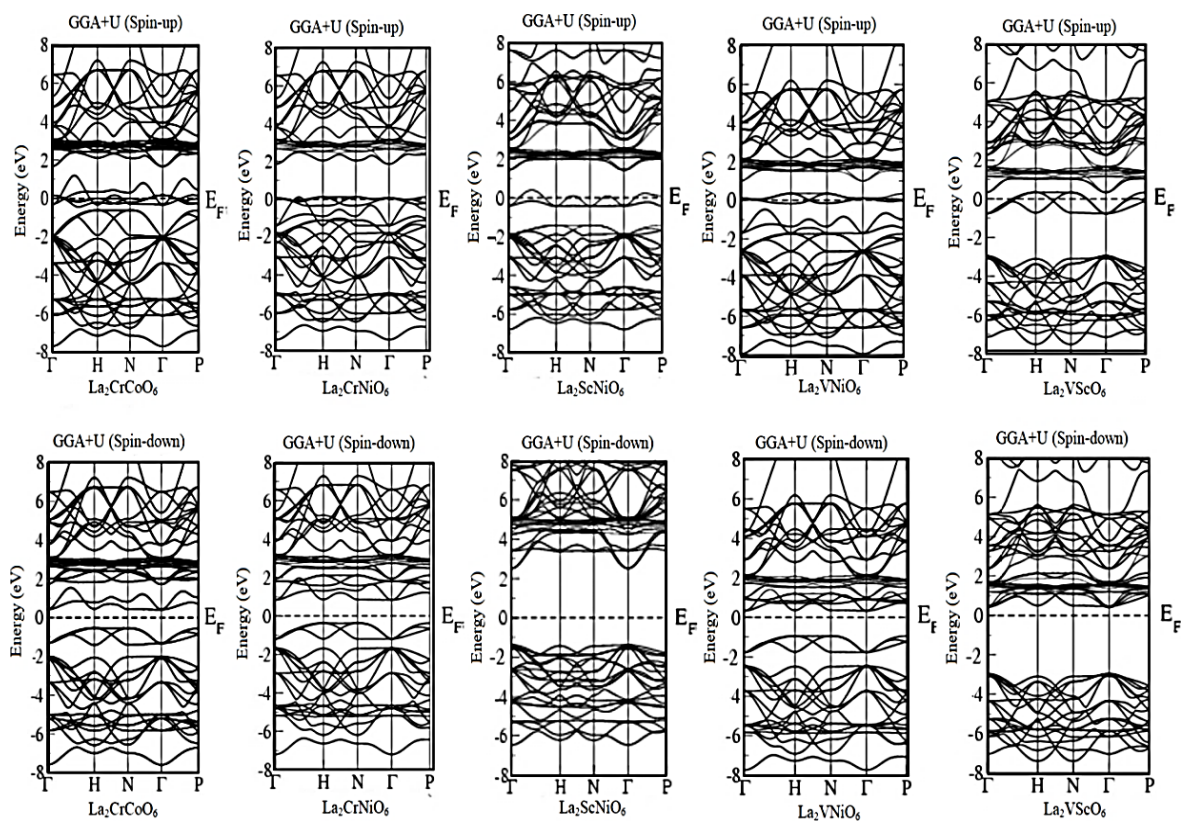


Figure 3. Band structures of DPC $\text{La}_2\text{BB}'\text{O}_6$ using GGA+U in both spin-up and spin-down channels.

3.2. Density of States Calculations

The density of states of the HM-DPCs describe the behaviour of the band structures, the electronic distribution is described in the form of the total density of states (TDOS) using GGA and GGA+U, as shown in Figures 4–8. All the DPC compounds are metallic for the spin-up channel and semiconductors for the spin-down channel in both the GGA and GGA+U schemes. The VB and CB overlap for the spin-up channel and for the spin-down channel there is an energy gap E_g between them. The negative side of energy describes VB, while the positive energy side shows CB, separated by the Fermi level E_f .

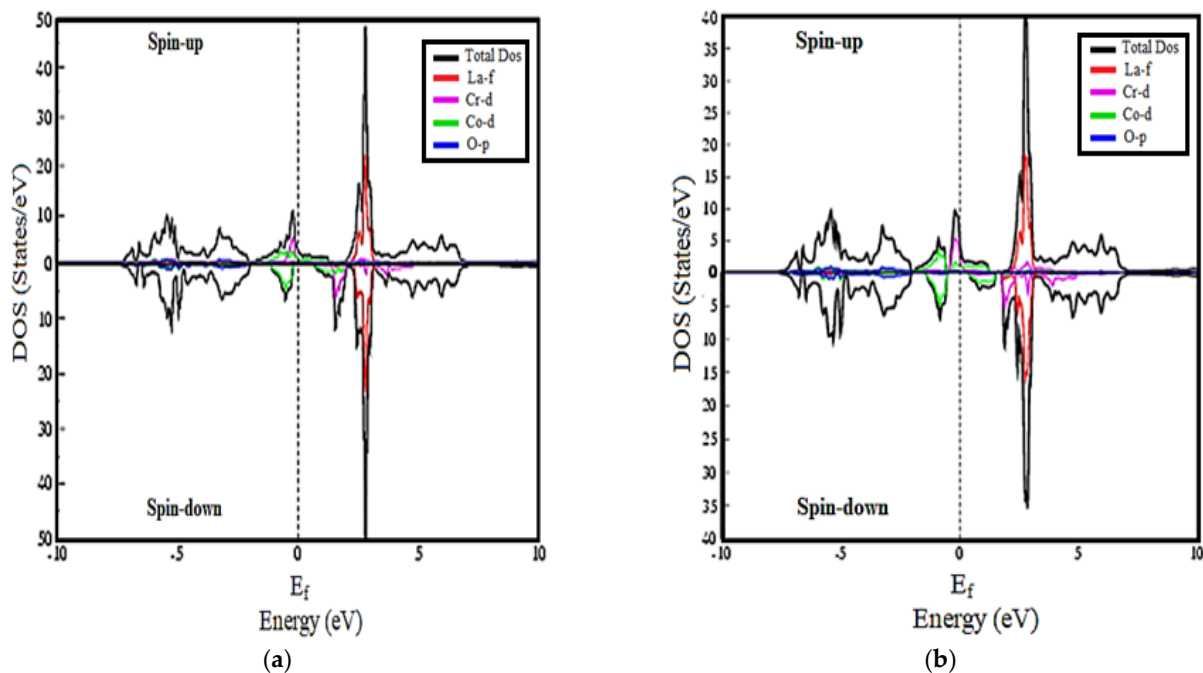


Figure 4. Density of states (DOS) of $\text{La}_2\text{CrCoO}_6$ using (a) GGA and (b) GGA+U.

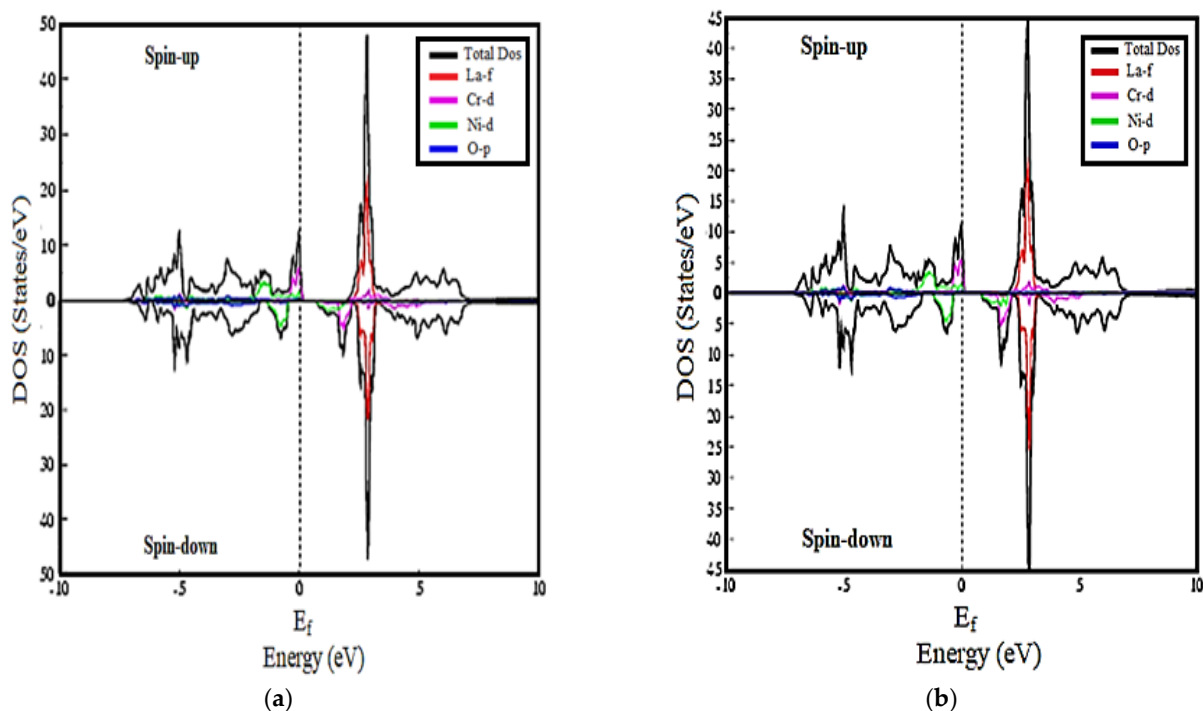


Figure 5. Density of states (DOS) of $\text{La}_2\text{CrNiO}_6$ using (a) GGA and (b) GGA+U.

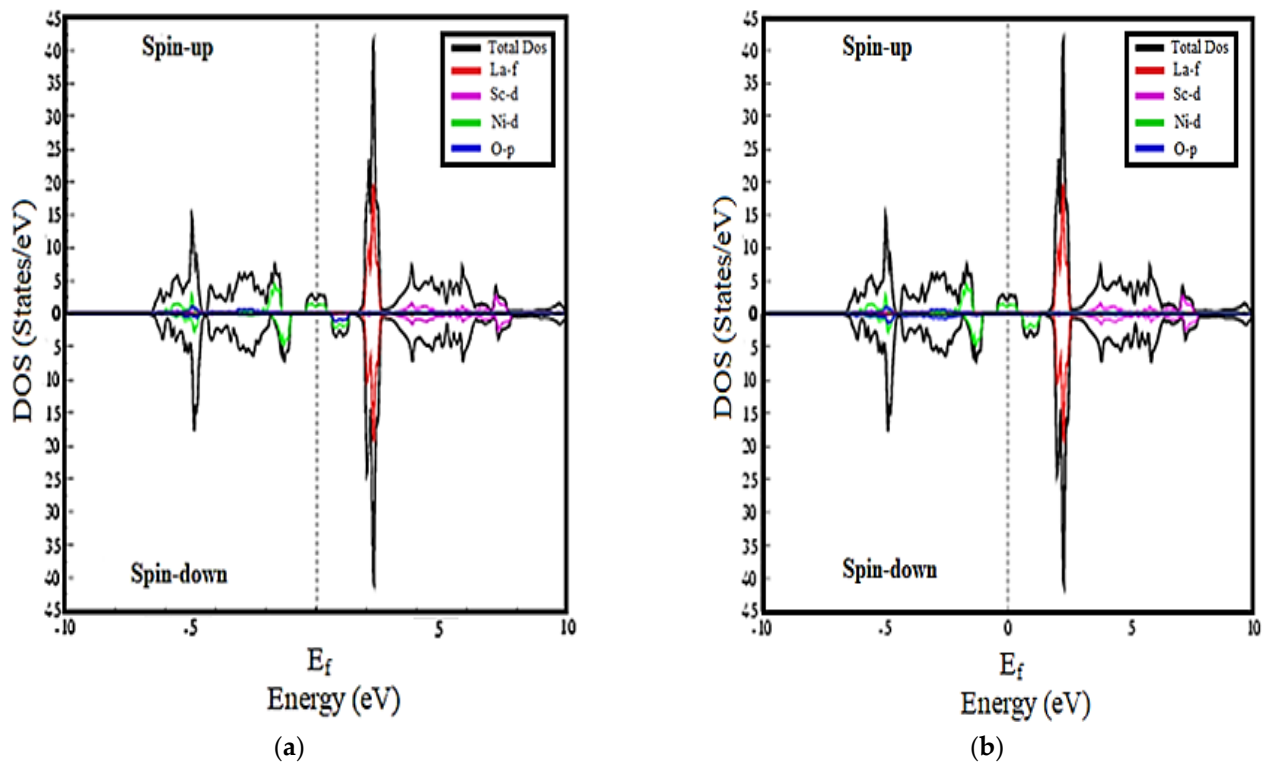


Figure 6. Density of states (DOS) of $\text{La}_2\text{ScNiO}_6$ using (a) GGA and (b) GGA+U.

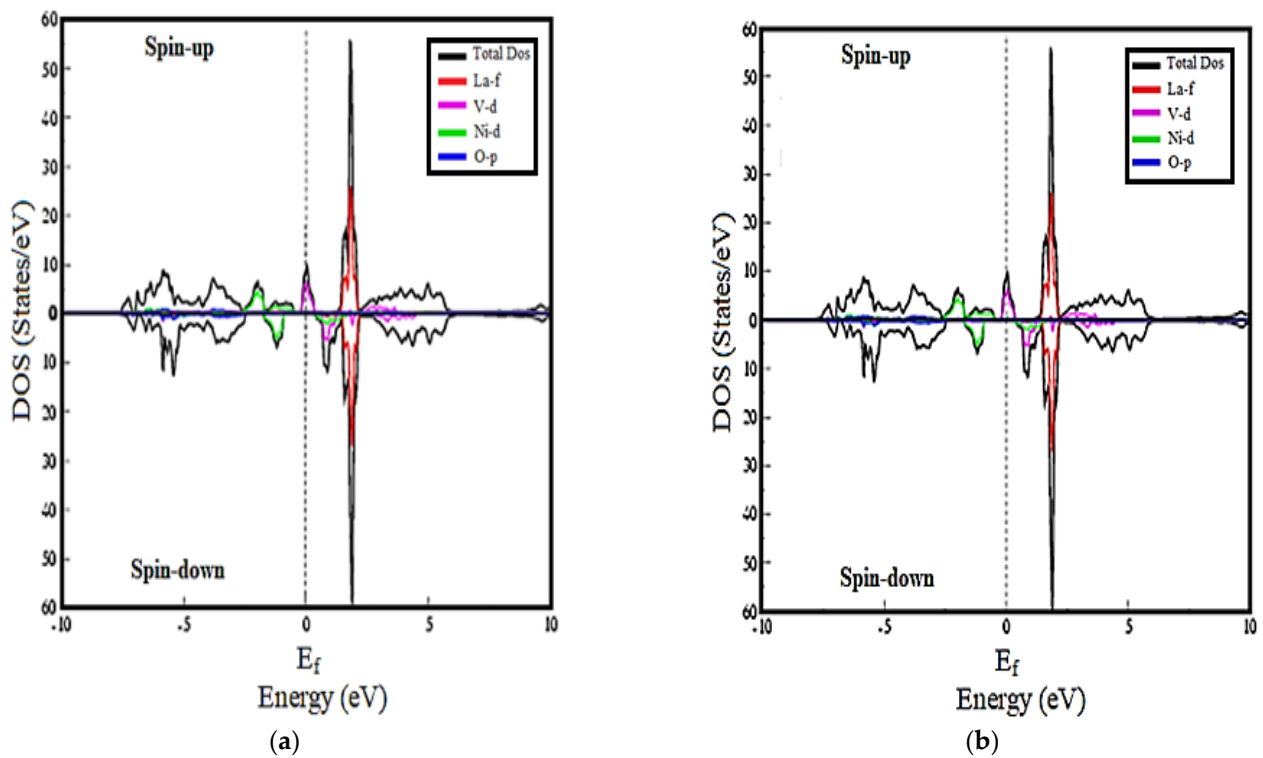


Figure 7. Density of states (DOS) of La_2VNiO_6 using (a) GGA and (b) GGA+U.

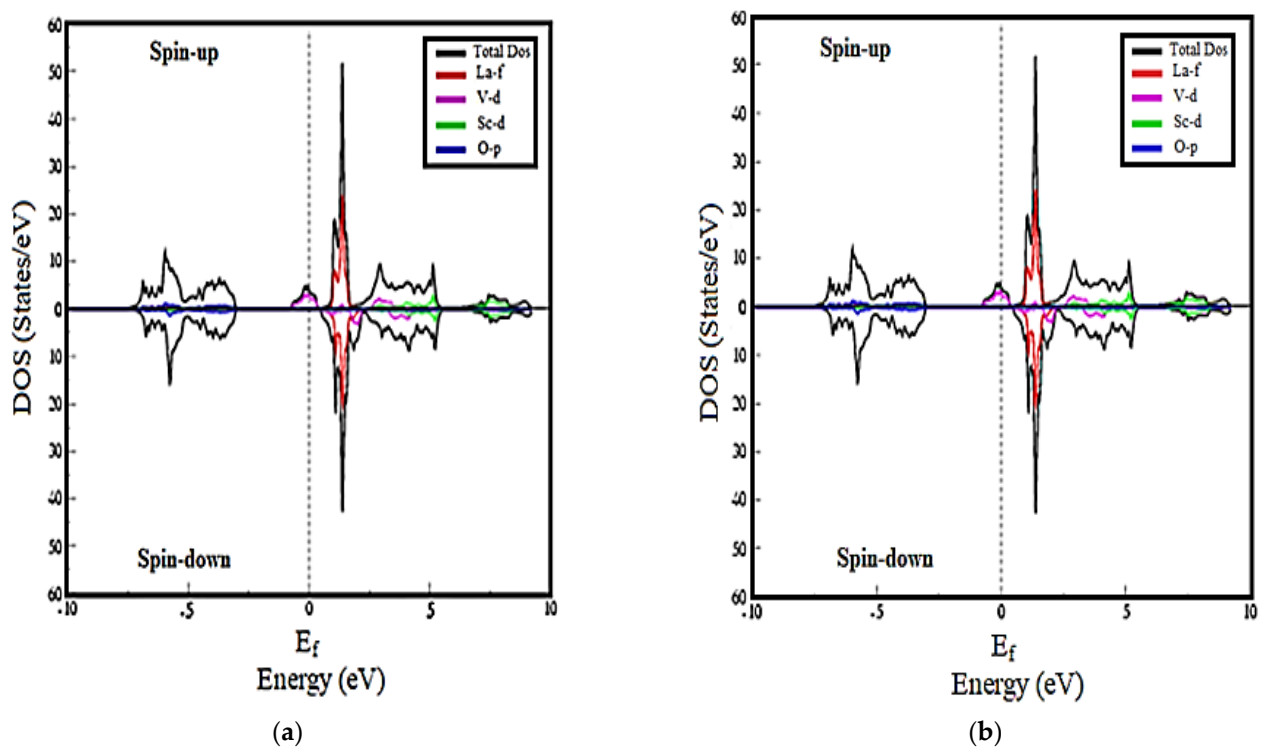


Figure 8. Density of states (DOS) of La_2VScO_6 using (a) GGA and (b) GGA+U.

For the compound $\text{La}_2\text{CrCoO}_6$ in the spin-down channel, the main contribution in VB is due to the Co-d orbital. The minor contribution of Cr-d is detected in the tVB and some congested peaks of O-p are also detected but too far from the edge of the VB. Inside the CB the Co-d is also found to be dominant near the edge and the major contribution of La-f is detected in the form of the high peaks shown in Figure 4a,b in GGA and GGA+U, respectively. For the compound $\text{La}_2\text{CrNiO}_6$ in the spin-down channel, the VB mostly consists of the tNi-d orbital and the CB consists of the Ni-d, Cr-d and La-f orbitals, as shown in Figure 5a,b. In the compound $\text{La}_2\text{ScNiO}_6$, the VB is mostly from the Ni-d orbital and a minor contribution of O-p is detected far away from the Fermi level E_f . The CB mostly consists of La-f orbitals and orbitals of the transition metals Ni and Sc. Looking towards La_2VNiO_6 , the VB mostly consists of the Ni-d orbital and the CB is crowded due to La-f and V-d towards E_f . In the final compound La_2VScO_6 , the VB is almost totally occupied by oxygen O-p and the CB is due to La-f, V-d and Sc-d. Overall, all the compounds are semiconductors in the spin-down channel and metallic in the spin-up channel. The main reason for their half-metallic nature is due to p-d hybridisation, the d-state pushes the p-state upward in the spin-down channel which separates E_f in different channels. Consequently, TDOS suggests that all compounds are half-metallic (HM) in which the VB is almost governed by transition metals (V, Sc, Ni, Co, Cr) and the CB is governed by Lanthanum La.

3.3. Magnetic Properties Calculations

For the investigation of the magnetic properties of the DPC $\text{La}_2\text{BB}'\text{O}_6$, the calculations are carried out in a spin-polarised manner in both the GGA and GGA+U schemes. The total spin magnetic moments are investigated and it was found that all the DPCs are half-metallic ferromagnetic (HM-FM) in nature. The total spin magnetic moment m^{cell} of the DPCs using GGA are $2.883 \mu_B$, $4.000 \mu_B$, $0.998 \mu_B$, $2.971 \mu_B$ and $2.008 \mu_B$ for $\text{La}_2\text{CrCoO}_6$, $\text{La}_2\text{CrNiO}_6$, $\text{La}_2\text{ScNiO}_6$, La_2VNiO_6 and La_2VScO_6 , respectively. Furthermore, using GGA+U, the total magnetic moments of the DPCs are $3.007 \mu_B$, $4.006 \mu_B$, $1.000 \mu_B$, $2.972 \mu_B$ and $2.010 \mu_B$ for $\text{La}_2\text{CrCoO}_6$, $\text{La}_2\text{CrNiO}_6$, $\text{La}_2\text{ScNiO}_6$, La_2VNiO_6 and La_2VScO_6 , respectively. The total spin magnetic moment of $\text{La}_2\text{CrNiO}_6$ is found to be high as compared to the other compounds

while the total spin magnetic moment of $\text{La}_2\text{ScNiO}_6$ is found to be minimum, which is $0.9 \mu_B$ and $1.000 \mu_B$ in both GGA and GGA+U, respectively. The spin magnetic moment measurements, atoms, interstitial region and total magnetic moment of the cell are given in Tables 2 and 3.

Table 2. Calculated spin magnetic moments of DPCs Using Generalised gradient approximation (GGA).

DPC	m^{INTERS}	m^{S1}	m^{S2}	m^{S3}	m^{S4}	m^{S5}	$m^{\text{Cell}} (\mu_B)$
$\text{La}_2\text{CrCoO}_6$	0.271	0.012	2.325	0.184	0.013	0.012	$2.883 \mu_B$
$\text{La}_2\text{CrNiO}_6$	0.282	0.014	1.998	1.389	0.048	0.050	$4.000 \mu_B$
$\text{La}_2\text{ScNiO}_6$	0.011	−0.002	0.045	0.776	0.028	0.028	$0.998 \mu_B$
La_2VNiO_6	0.153	0.013	0.892	1.481	0.069	0.069	$2.971 \mu_B$
La_2VScO_6	0.427	0.073	1.423	0.036	−0.004	−0.004	$2.008 \mu_B$

Table 3. Calculated spin magnetic moments of DPCs Using Generalised gradient approximation with hybrid term (GGA+U).

DPC	m^{INTERS}	m^{S1}	m^{S2}	m^{S3}	m^{S4}	m^{S5}	$m^{\text{Cell}} (\mu_B)$
$\text{La}_2\text{CrCoO}_6$	0.323	0.021	2.388	0.154	0.018	0.015	$3.007 \mu_B$
$\text{La}_2\text{CrNiO}_6$	0.263	0.012	1.974	1.402	0.056	0.057	$4.006 \mu_B$
$\text{La}_2\text{ScNiO}_6$	−0.016	0.002	0.017	1.319	−0.057	−0.052	$1.000 \mu_B$
La_2VNiO_6	0.153	0.013	0.895	1.483	0.068	0.069	$2.972 \mu_B$
La_2VScO_6	0.429	0.073	1.427	0.036	−0.005	−0.005	$2.010 \mu_B$

3.4. Optical Properties Calculations

The optical characteristic absorption coefficient and optical conductivity are calculated for all DPCs. Figure 9a,b shows the absorption coefficient of the DPCs using GGA and GGA+U.

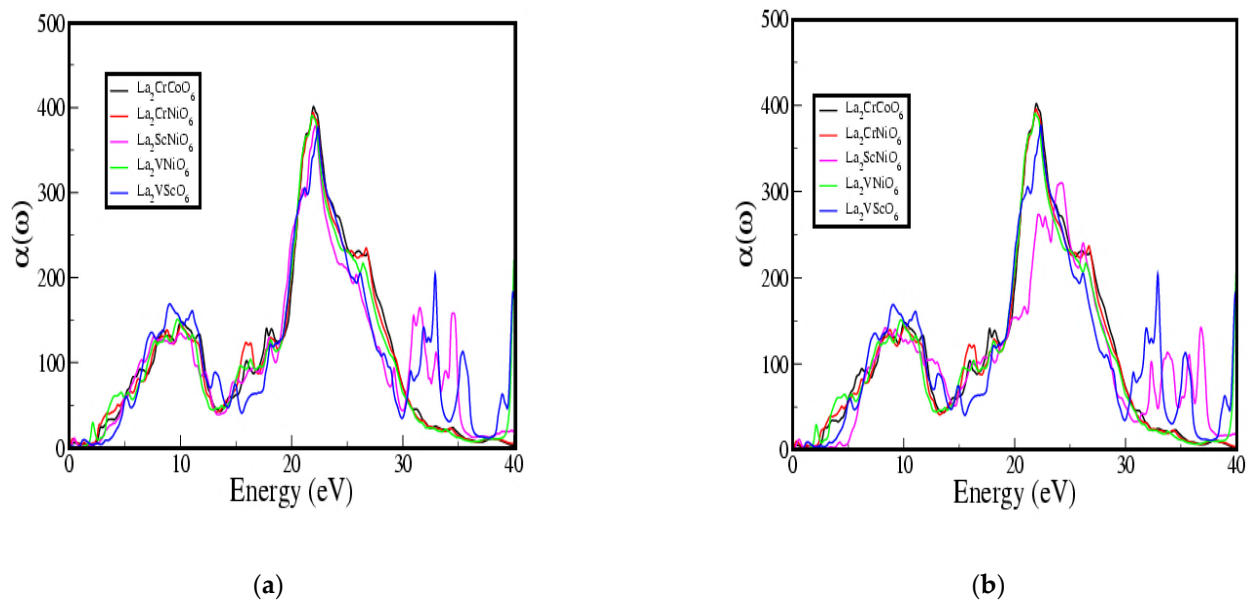


Figure 9. (a) Absorption coefficient of DPCs $\text{La}_2\text{BB}'\text{O}_6$ using GGA and (b) using GGA+U.

The absorption coefficient $\alpha(\omega)$ of all the DPCs is plotted and the energy is taken from 0–40 eV against $\alpha(\omega)$. All compounds absorb wavelengths of energy when the energy increases from 1 eV. Within the visible energy limit, the La_2VNiO_6 absorbs much more wavelengths and, in the range of 0–40 eV, the compound $\text{La}_2\text{CrCoO}_6$ has outstanding behaviour. The higher peak of 401.082 at the energy of 21.9 eV is detected. Likewise, the

compound La_2VScO_6 shows suitable behaviour as a light-absorbing material. The results of the absorption coefficient in both schemes, GGA and GGA+U are almost the same. The maximum absorption shift occurs in between the energy range of 20–25 eV, therefore these compounds can be used as absorbers in many electronic applications.

The optical conductivity $\sigma(\omega)$ describes the behaviour of the DPCs in the presence of energy (eV). Within the visible range, all compounds show suitable conductivity, and the compound La_2VNiO_6 shows good conductivity in the visible region. When the energy is increasing the $\sigma(\omega)$ of the compounds increases, the compound $\text{La}_2\text{CrCoO}_6$ shows the maximum conductivity, which is 14,950 at 21 eV. The optical conductivity of all compounds increased when the energy increased from 18–21 eV, as shown in Figure 10a,b. All the compounds were found to be good optical conductors that could be used in perovskite solar cells as absorbers.

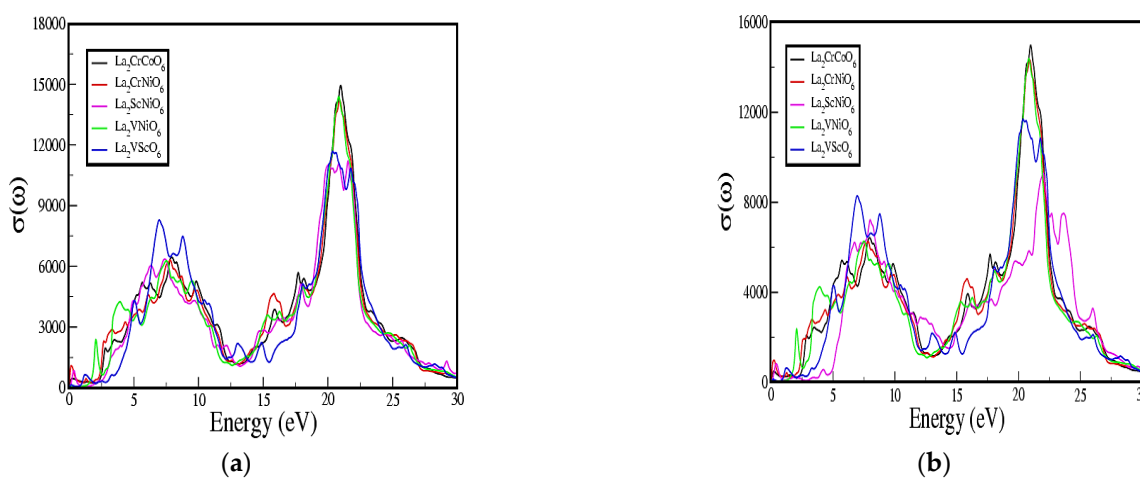


Figure 10. (a) Optical conductivity of DPC $\text{La}_2\text{BB}'\text{O}_6$ using GGA and (b) GGA+U.

Due to the versatile behaviour of these compounds—electronic, magnetic and optical—they are the best candidates for electronic and spintronic applications.

4. Conclusions

In summary, we calculated the electronic, magnetic and optical properties of $\text{La}_2\text{BB}'\text{O}_6$ where $B = \text{Cr}, \text{Sc}$ and V and $B' = \text{Co}, \text{Ni}$ using a first principle DFT approach. The DPCs were metallic for the spin-up channel B' and showed semiconductor behaviour for the spin-down channel. For the spin-up channel, the VB and CB overlap and for the spin-down channel, there is an energy gap E_g between them. The E_g of the DPC agrees but is only a little higher as compared to the previous theoretical findings due to higher symmetry and enhanced optimisation. The VB and CB mainly consist of transition metal d-states and lanthanum-f states, respectively. The magnetic properties suggest that all DPC compounds are ferromagnetic (FM). Therefore, all the DPCs are half-metallic ferromagnetic (HM-FM) in nature. The DPCs show good optical properties such as their absorption coefficient and optical conductivity. Furthermore, the compound $\text{La}_2\text{CrCoO}_6$ showed phenomenal electronic and optical properties to its narrow band gap in the spin-down channel. These compounds are suggested for spintronic applications due to their half-metallic ferromagnetic (HM-FM) character.

Author Contributions: Conceptualisation, M.U.R. and Q.W.; methodology, M.U.R.; software, Q.W.; investigation, Y.Y.; writing, M.U.R. All authors have read and agreed to the published version of the manuscript.

Funding: This work was supported by the National Key Research and Development Program of China (No. 2018YFF01013601).

Institutional Review Board Statement: Not applicable.

Informed Consent Statement: Not applicable.

Data Availability Statement: All data generated or analysed during this study are included in this published article.

Conflicts of Interest: The authors declare no conflict of interest.

References

1. Sarma, D.D. A new class of magnetic materials: $\text{Sr}_2\text{FeMoO}_6$ and related compounds. *Curr. Opin. Solid State Mater. Sci.* **2001**, *5*, 261–268. [[CrossRef](#)]
2. Vasala, S.; Karppinen, M. $\text{A}_2\text{B}'\text{B}''\text{O}_6$ perovskites: A review. *Prog. Solid State Chem.* **2015**, *43*, 1–36. [[CrossRef](#)]
3. Mahesh, R.; Kannan, K.R.; Rao, C.N.R. Electrochemical synthesis of ferromagnetic LaMnO_3 and metallic NdNiO_3 . *J. Solid State Chem.* **1995**, *114*, 294–296. [[CrossRef](#)]
4. Sleight, A.W.; Gillson, J.L.; Bierstedt, P.E. High-temperature superconductivity in the $\text{BaPb}_{1-x}\text{Bi}_x\text{O}_3$ system. *Solid State Commun.* **1993**, *88*, 841–842. [[CrossRef](#)]
5. MacChesney, J.B.; Sherwood, R.C.; Potter, J.F. Electric and magnetic properties of the strontium ferrates. *J. Chem. Phys.* **1965**, *43*, 1907–1913. [[CrossRef](#)]
6. Aylett, B.J. *Transition Metal Oxides: Structure, Properties and Synthesis of Ceramic Oxides*, 2nd ed.; Rao, C.N.R., Raveau, B., Eds.; Wiley-VCH: New York, NY, USA; Weinheim, Germany, 1998; p. 80; ISBN 0-471-18971-5.
7. Hikami, S.; Matsuda, Y. High Tc superconductors of the perovskite structure oxides. *Jpn. J. Appl. Phys.* **1987**, *26*, 1027. [[CrossRef](#)]
8. Bhalla, A.S.; Guo, R.; Roy, R. The perovskite structure—A review of its role in ceramic science and technology. *Mater. Res. Innov.* **2000**, *4*, 3–26. [[CrossRef](#)]
9. Saha-Dasgupta, T. Double perovskites with 3d and 4d/5d transition metals: Compounds with promises. *Mater. Res. Express* **2020**, *7*, 014003. [[CrossRef](#)]
10. Galasso, F.; Pyle, J. Ordering in compounds of the $\text{A}(\text{B}'0.33\text{Ta}0.67)\text{O}_3$ type. *Inorganic Chem.* **1963**, *2*, 482–484. [[CrossRef](#)]
11. Lemmens, P.; Millet, P. Spin—Orbit—Topology, a triptych. *Quantum Magn.* **2004**, *645*, 433–477.
12. Wu, H. Electronic structure study of double perovskites A_2FeReO_6 ($\text{A} = \text{B a, S r, C a}$) and $\text{Sr}_2\text{M MoO}_6$ ($\text{M} = \text{C r, M n, F e, C o}$) by LSDA and LSDA+ U. *Phys. Rev. B* **2001**, *64*, 125126. [[CrossRef](#)]
13. Jin, X.; Wang, Q.; Jadoon, A.M. Opto-Electronic Properties of Methyl-Ammonium Lead Halide: A First Principle Approach. In *Journal of Physics: Conference Series*; IOP Publishing: Bristol, UK, 2020; Volume 1622, p. 012105.
14. Ghaithan, H.M.; Alahmed, Z.A.; Qaid, S.M.; Aldwayyan, A.S. Density Functional Theory Analysis of Structural, Electronic, and Optical Properties of Mixed-Halide Orthorhombic Inorganic Perovskites. *ACS Omega* **2021**, *6*, 30752–30761. [[CrossRef](#)] [[PubMed](#)]
15. Kabbour, H.; Gauthier, G.H.; Tessier, F.; Huvé, M.; Pussacq, T.; Roussel, P.; Mentre, O. Topochemical reduction of YMnO_3 into a composite structure. *Inorg. Chem.* **2017**, *56*, 8547–8553. [[CrossRef](#)] [[PubMed](#)]
16. Jeng, H.T.; Guo, G.Y. First-principles investigations of orbital magnetic moments and electronic structures of the double perovskites $\text{Sr}_2\text{FeMoO}_6$, $\text{Sr}_2\text{FeReO}_6$, and Sr_2CrWO_6 . *Phys. Rev. B* **2003**, *67*, 094438. [[CrossRef](#)]
17. Holman, K.L.; Huang, Q.; Klimczuk, T.; Trzebiatowski, K.; Bos, J.W.G.; Morosan, E.; Cava, R.J. Synthesis and properties of the double perovskites La_2NiVO_6 , La_2CoVO_6 , and $\text{La}_2\text{CoTiO}_6$. *J. Solid State Chem.* **2007**, *180*, 75–83. [[CrossRef](#)]
18. Alias, F.I.H.; Maulud, M.F.; Mohamed, Z. Structural and optical properties of tellurium-based double perovskite $\text{Sr}_2\text{ZnTeO}_6$. In *AIP Conference Proceedings*; AIP Publishing LLC: New York, NY, USA, 2021; Volume 2368, p. 030001.
19. Neelu, N.; Pandey, N.; Chakrabarti, S. Synthesis and optical study of ultra stable inorganic double perovskite $\text{Cs}_2\text{CuBiCl}_6$ for optoelectronic applications. In *Proceedings of the Organic, Hybrid, and Perovskite Photovoltaics XXIII*, San Diego, CA, USA, 22 August 2022; Volume 12209, pp. 39–45.
20. Malyshkin, D.; Novikov, A.; Ivanov, I.; Sereda, V.; Tsvetkov, D.; Zuev, A. The origin of triple conductivity and water uptake in layered double perovskites: A case study on lanthanum-substituted $\text{GdBaCo}_2\text{O}_{6-\delta}$. *J. Alloys Compd.* **2020**, *845*, 156309. [[CrossRef](#)]
21. Bhowmik, T.K.; Sheikh, M.S.; Sakhya, A.P.; Dutta, A.; Sinha, T.P. Synthesis, structural and electrical conductivity of half-metallic perovskite oxide $\text{La}_2\text{CrNiO}_6$. In *AIP Conference Proceedings*; American Institute of Physics: College Park, MD, USA, 2021; Volume 2369, p. 020080.
22. Perdew, J.P. Density-functional approximation for the correlation energy of the inhomogeneous electron gas. *Phys. Rev. B* **1986**, *33*, 8822. [[CrossRef](#)]
23. Schwarz, K. DFT calculations of solids with LAPW and WIEN2k. *J. Solid State Chem.* **2003**, *176*, 319–328. [[CrossRef](#)]
24. Schwarz, K.; Blaha, P.; Trickey, S.B. Electronic structure of solids with WIEN2k. *Mol. Phys.* **2010**, *108*, 3147–3166. [[CrossRef](#)]
25. Slater, J.C. *Introduction to Chemical Physics*; Read Books Ltd.: Redditch, UK, 2011.
26. Anisimov, V.I.; Zaanen, J.; Andersen, O.K. Band theory and Mott insulators: Hubbard U instead of Stoner I. *Phys. Rev. B* **1991**, *44*, 943. [[CrossRef](#)]
27. Liu, Y.P.; Chen, S.H.; Fuh, H.R.; Wang, Y.K. First-principle calculations of half-metallic double perovskite La_2BBO_6 (B , $\text{B} = 3\text{d}$ transition metal). *Commun. Comput. Phys.* **2013**, *14*, 174–185. [[CrossRef](#)]